J Physiol (2003), **553.2**, *pp.* 561–574

DOI: 10.1113/jphysiol.2003.043257
www.jphysiol.org

Journal of Physiology

Role of villus microcirculation in intestinal absorption of glucose: coupling of epithelial with endothelial transport

J. R. Pappenheimer and C. C. Michel *

*Department of Biology, Harvard University, Cambridge, MA, USA and * Division of Biomedical Sciences, Faculty of Medicine, Imperial College, Exhibition Road, London SW7 2AZ, UK*

Capillaries in jejunal villi can absorb nutrients at rates several hundred times greater (per gram tissue) than capillaries in other tissues, including contracting skeletal muscle and brain. We here present an integrative hypothesis to account for these exceptionally large trans-endothelial fluxes and their relation to epithelial transport. Equations are developed for estimating concentration gradients of glucose across villus capillary walls, along paracellular channels and across subjunctional lateral membranes of absorptive cells. High concentrations of glucose discharged across lateral membranes to subjunctional intercellular spaces are delivered to abluminal surfaces of villus capillaries by convection–diffusion in intercellular channels without significant loss of concentration. Post-junctional paracellular transport thus provides the series link between epithelial and endothelial transport and makes possible the large trans-endothelial concentration gradients required for absorption to blood. Our analysis demonstrates that increases of villus capillary blood flow and permeability–surface area product (PS) are essential components of absorptive mechanisms: epithelial transport of normal digestive loads could not be sustained without concomitant increases in capillary blood flow and PS. The low rates of intestinal absorption found in anaesthetised animals may be attributed to inhibition of normal villus microvascular responses to epithelial transport.

(Received 20 March 2003; accepted after revision 18 August 2003; first published online 22 August 2003)
Corresponding author C. C. Michel: Sundial House, High Street, Alderney, Guernsey GY9 3UG, UK.
Email: c.c.michel@ic.ac.uk

In 1932, Dill, Edwards & Talbott described experiments in which dogs of 15 kg body weight ran up a gradient of 17 deg on a treadmill almost continuously for more than 24 h, stopping for only 5 min of each hour to ingest about 250 ml of water and 40 g (220 mmol) of sugar. The authors were interested in muscular fatigue and did not appreciate the significance of their experiments for mechanisms of intestinal absorption. The amounts of sugar absorbed each hour far exceeded the maximum rates of trans-cellular sugar absorption found in isolated preparations of intestine or in perfused intestinal segments in anesthetised animals. Nutrients absorbed by the epithelium must also be absorbed by capillaries in the lamina propria of the villi; when expressed per gram of jejunum the rates of absorption of glucose by villus capillaries in the experiments of Dill *et al.* (1932) were more than two orders of magnitude greater than flux in other tissues, including brain (Kety & Schmidt, 1948) and contracting skeletal muscle (Vock *et al.* 1996); when expressed per gram of absorbing tissue in the upper third of the villi the difference is more than 500-fold. Krogh (1929) stated the problem conservatively in his book *The Anatomy and Physiology of Capillaries* when he noted that in normal humans some 400 g sugar and 100 g amino acids are absorbed each day by the capillaries of villus tips weighing only a few grams. Pilots training for the human powered airplane ('Daedalus') ingested and absorbed glucose at the rate of 550 mmol h^{-1} for several hours (Nadel & Bussolari, 1988), a rate that implies an absorptive flux of more than 15 000 μmol h^{-1} (g villus tissue)$^{-1}$. Perfused segments of jejunum in normal (unanaesthetised) human subjects can absorb glucose at rates exceeding 4000 μmol h^{-1} (cm length of luminal catheter)$^{-1}$ (Holdsworth & Dawson, 1964; Gray & Inglefinger, 1965, 1966; Gisolfi *et al.* 1992) or about 10 000 μmol h^{-1} (gram villus tissue)$^{-1}$. In contrast, the flux of glucose across capillary walls in skeletal muscles of dogs running at 85 % of their aerobic capacity is only 20 μmol h^{-1} (gram muscle)$^{-1}$ (Vock *et al.* 1996).

In a preliminary paper, one of us (Pappenheimer, 2001*b*) called attention to some of these facts and offered a tentative hypothesis to explain them. It was estimated that the velocity of transport of fluid and glucose in inter-cellular channels is many times faster than transport by diffusion through the cytoplasm of enterocytes and this mechanism provides the high concentration of nutrients required for trans-endothelial diffusion into villus capillary blood. However, no attempt was made to develop the hypothesis in detail or to analyse the transcapillary phase of the absorption in terms of capillary surface area, concentration gradients and permeability.

The purpose of the present paper is to analyse these problems in detail. In Part I we present equations describing convection–diffusion in intercellular channels and across villus capillary endothelium, taking account of the shape and dimensions of the channels and the surface area and permeability of the capillaries. In Part II we examine morphological and functional data from the literature that are appropriate for insertion in the equations to estimate concentration gradients across lateral membranes of enterocytes, along paracellular channels and across villus capillary walls. In the results section (Part III) we show how transport across apical membranes of enterocytes is coupled in series with the villus microvascular system. The results indicate that responses of the microvascular system to glucose loading are at least as important as the epithelium in determining absorption rates of glucose in normal (unanaesthetised) animals.

Part I: convection and diffusion of sugars and amino acids in channels between absorptive cells of the small intestine

A clear picture of the transport pathways for glucose between the fluid at the luminal surface of the jejunal epithelial cells and the villus capillary blood is an essential starting point for a quantitative analysis of the transport processes. We begin by describing these pathways, recognising that some readers may regard them as controversial. In Part III, however, we show that the potentially controversial points are of minor consequence and do not influence our conclusions.

Sugars and amino acids generated by hydrolysis of saccharides and oligopeptides in the brush border are transported to subjunctional regions of intercellular channels through two different pathways . (1) They can be concentrated in apical cytoplasm of absorptive cells by specific Na^+-coupled membrane proteins (SLGT-1 in the case of glucose) and subsequently discharged to intercellular channels by facilitated diffusion on passive carriers in lateral membranes. In the case of glucose it has been demonstrated by Cheeseman (1992) and by Kellett (2001) that the passive carrier Glut-2 is a constituent of lateral membranes of absorptive cells and is mobilised to the terminal web during Na^+-coupled, concentrative transport to apical cytosol of glucose generated by membrane-bound hydrolases of the microvilli. (2) Sugars and amino acids (as well as small inert solutes that cannot pass cell membranes) also reach intercellular channels by solvent drag through intercellular junctions that are dilated by perijunctional contractile proteins during fluid absorption induced by Na^+-coupled transport (Pappenheimer & Reiss, 1987; Madara & Pappenheimer, 1987; Sadowski & Meddings, 1993; Karasov & Cork, 1994; Nusrat *et al.* 2000). The energy for establishing transjunctional osmotic flow and paracellular transport of solutes is derived from hydrolysis of ATP as Na^+ brought to apical cytosol with SLGT-1 is pumped out laterally. The ATP-ase is located in lateral membranes below the junctions (Amerongen *et al.* 1989). Between 50 and 70 % of fluid absorption occurs through intercellular junctions as estimated from clearances of inert solutes or from clearances of hexoses after saturation of their transporters (Pappenheimer & Reiss, 1987; Pappenheimer, 2001*a*).

Intracellular convection and diffusion from apical to basal cytoplasm of absorptive cells is obstructed by their nuclei, mitochondria, endoplasmic reticulum and other intracellular membranous structures (Buschman & Manke, 1981; Buschman, 1983; Madara & Trier, 1994); the nucleus

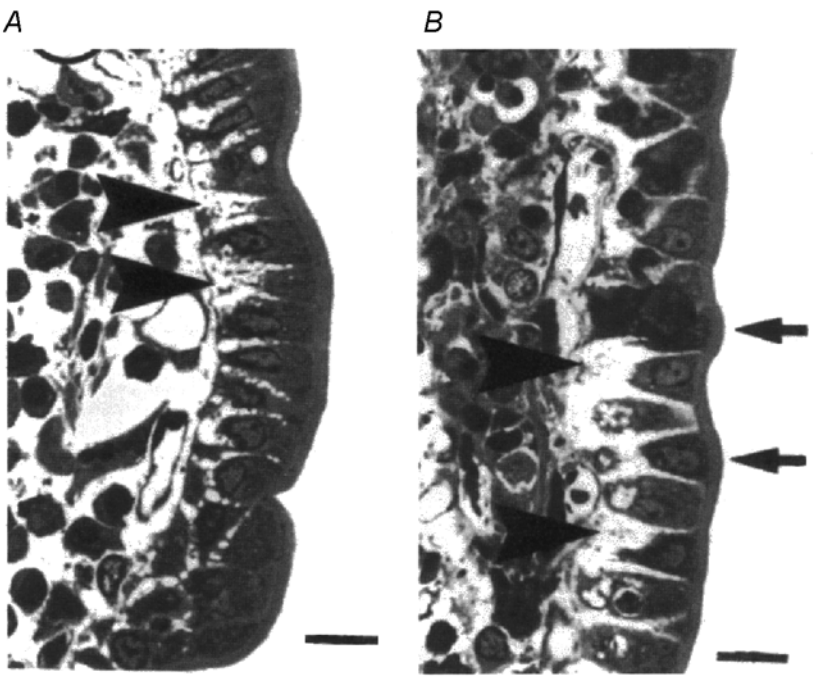

Figure 1. Light micrographs of 1 μm sections of villus epithelium fixed rapidly during the perfusion of hamster jejunum with 25 mM glucose

A, isolated segments of jejunum where the lumen was perfused with glucose *in vitro*. *B*, jejunum of an anaesthetised animal where the gut lumen was perfused with glucose and its wall supplied with an intact circulation right up to the time of fixation. Note conical absorptive cells and intercellular spaces (large arrowheads) with capillaries immediately below the basement membrane. Average dimensions of the channels are presented in Table 1. Scale bar at bottom right of each micrograph is 20 μm. (Reproduced with permission from Madara & Pappenheimer, 1987).

alone occupies most of the cross-sectional area of each absorptive cell and it seems unlikely that large fluxes of fluid and organic solutes can pass through the intracellular membranes and concentrated contents of nuclei or mitochondria. We assume, therefore, that hydrophilic nutrients concentrated in apical cytosol are discharged to intercellular channels located in subjunctional regions of the terminal web. It follows that the post-junctional paracellular channels provide the principal pathway for transport of nutrients from apical regions of absorptive cells to capillaries in the lamina propria of the villi. In the following analysis we estimate the contributions of convection (solvent drag) and diffusion to the transport of glucose from subjunctional regions of intercellular channels to the vicinity of capillaries adjacent to the basement membrane of absorptive cells in the lamina propria of the villi. Our analysis includes estimation of the concentration gradient of glucose across apical regions of lateral membranes of absorptive cells and the concentration of glucose in basal extracellular fluid required to drive glucose across capillary membranes.

Flow velocity in intercellular channels varies inversely with the cross-sectional area of the channels whereas diffusion varies in proportion to the area; it follows that the shape and dimensions of the channels must be specified in order to estimate the relative roles played by convection and diffusion. The fact that intercellular channels between absorptive cells are widened during Na^+-coupled transport of sugars and amino acids was demonstrated histologically in hamster jejunum by Madara & Pappenheimer (1987) and subsequently confirmed by measurements of trans-mucosal impedance (Pappenheimer & Volpp, 1992) and by direct visualisation of fluorescein by confocal scanning microscopy (Chang, 2002). During Na^+-coupled absorption of glucose or alanine the enterocytes lose about 30 % of their fluid to intercellular space (Pappenheimer, 2001*b*); the cells take the (approximate) form of truncated cones with their widest diameter at the apex and their smallest at the basal membrane as illustrated in Figs 1 and 2. Horizontal cross-sections of absorptive cells at the level of junctions are polygonal rather than circular as shown in Fig. 10 of the paper by Madara & Pappenheimer (1987). This honeycomb shape permits tight packing at the level of junctions whereas circular cross-sections would present more than 15 % of the area as open channels facing the lumen of the intestine. Widening of intercellular channels begins below tight junctions, as indicated in Fig 1. To simplify calculations we assume that horizontal cross-sections of absorptive cells are circular below the terminal web. Although the theory to be developed will be applied specifically to glucose, it may be applied to any sugar or amino acid for which there is adequate flux data.

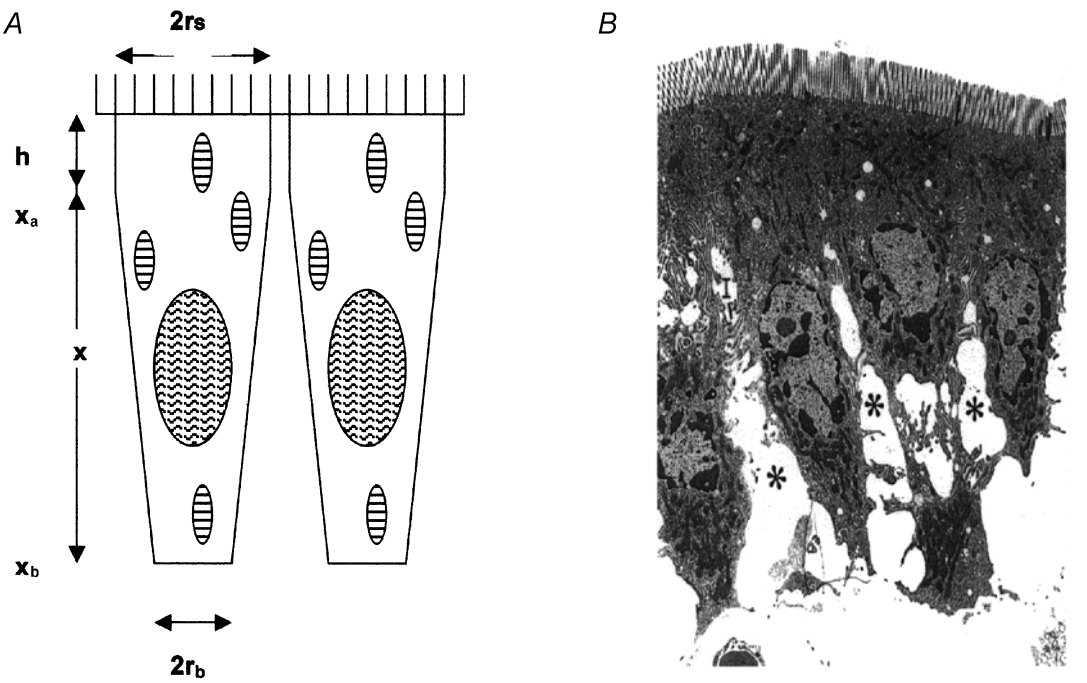

Figure 2. Dimensions of the absorbing enterocytes

Figure 2*A* defines the dimensions used to construct Table 1.The apical parts of epithelial cells are considered as cylinders of radius r_S and depth h and the middle and basal parts of the cells as inverted truncated cones with radii r_S and r_b, extending from the basal aspect of the tight junction at x_a to basement membrane at x_b. Figure 2*B* is a low-power electron micrograph of hamster jejunal cells fixed rapidly during the absorption of glucose; the asterisks indicate the widened lateral intercellular spaces. (Reproduced with permission from Madara & Pappenheimer, 1987).

The concentration of glucose in intercellular channels. The basic equation for convection and diffusion through a channel of cross-sectional area, A, and length, x, is

$$J_S = J_V C - DA\,(dC/dx), \quad (1)$$

where J_s is the flux of solute, J_v is the flow of solvent, D is the diffusion coefficient and dC/dx is the (negative) slope of the gradient at any distance, x. In a channel of constant cross-sectional area, A_o, and length, x_o, integration of eqn (1) takes the form:

$$J_S = J_V \frac{\{C_a - C_b \exp[-(J_V x_o/DA_o)]\}}{1 - \exp[-(J_V x_o/DA_o)]}, \quad (2)$$

where C_a is the concentration at the entrance to the channel and C_b is the concentration at its exit.

The dimensionless exponent $-(J_v x_o/DA_o)$ is known as the Péclet number (Denbigh, 1965).

Equation (2) has been utilised to analyse thickness of unstirred layers in frog skin (Dainty & House, 1966) and in the small intestine (Gruzdkov *et al.* 1989; Pappenheimer, 2001*a*) but in the present case the cross-sectional area of the channels increases approximately with the square of the distance and integration of eqn (1) is more complex. The solution of eqn (1) for a channel of variable area can be written in the same form as eqn (2) but with a variable Péclet number (p) as the exponent. Thus,

$$J_S = J_V \frac{[C_a - C_b \exp(-p)]}{1 - \exp(-p)}, \quad (3)$$

where

$$p = \frac{J_V}{D} \int_{x=a}^{x=b} \frac{dx}{A_x}.$$

The subjunctional glucose concentration at the entrance to the intercellular channels (C_a) is then:

$$C_a = C_b \exp(-p) + \frac{J_S}{J_V}[1 - \exp(-p)]. \quad (3a)$$

The concentration difference from just beneath the tight junction at $x = a$ to the basement membrane at $x = b$ is

$$C_a - C_b = \left(\frac{J_S}{J_V} - C_b\right)[1 - \exp(-p)]. \quad (3b)$$

For channels between the conical cells, illustrated in Fig. 2*A*, the integral of the exponent (Péclet number, p) in eqns (3*a*) and (3*b*) is

$$p = (J_V/D)\,[(r_s x_b)10^{-4}/2(r_s - r_b)]\,\ln[2r_s x_b - (r_s - r_b)x_a] / (r_s + r_b)x_a, \quad (4)$$

where p refers to the channel area relative to smooth apical surface area of enterocytes and r_s and r_b represent the radii of the cell at x_a and x_b, respectively. When referred to the smooth luminal surface area of the jejunum, $p' = p/2$ in rats and $p/3$ in humans as described below in the paragraph on surface areas of villi and capillaries. The dimensions of cells and channels (r_s, r_b and x_b) are given in Table 1 and x_a is taken at a point 10 % of the distance from the tight junction to the basement membrane. Since the cell nucleus, mitochondria and other intracellular membrane structures obstruct transport through most of the cytoplasm, we assume that all or most of the glucose flux passes preferentially on Glut-2 through the upper 10 % of the subjunctional lateral membranes. Details of the integration leading to eqn (4) and a sample numerical calculation of p are given in the Appendix. A similar integral form of the Péclet number was used in eqn (13) of the paper by Koefoed-Johnsen & Ussing (1953) to describe flow and diffusion of D_2O through the epithelium of frog skin.

The concentration of glucose at the basement membrane adjacent to the abluminal surface of villus capillaries, C_b. Numerical solutions to eqns (3*a*) and (3*b*) require knowledge of C_b, the concentration of glucose at or near the abluminal surface of villus capillaries immediately adjacent to the basement membrane of epithelial cells. C_b can be evaluated by the following analysis.

As blood flows along villus capillaries of length L, the flux of glucose entering the blood at any distance l, is

$$J_S = \mathrm{PS}\frac{dl}{L}(C_b - C_l) = Q_b dC_l \text{ or } \frac{dl}{L} = \frac{\dot{Q}_b}{\mathrm{PS}} \frac{dC_l}{(C_b - C_l)}, \quad (5)$$

where C_l represents the mean luminal concentration of glucose, PS represents permeability–surface area product and $\dot{Q}_b$ represents capillary blood flow, both measured in $cm^3\,h^{-1}$.

After integration between $l = 0$ and $l = L$ and solving for C_b

$$C_b = \frac{(C_V \exp(\mathrm{PS}/\dot{Q}_b) - C_{art})}{(\exp(\mathrm{PS}/\dot{Q}_b) - 1)}, \quad (6)$$

where C_V represents the glucose concentration in venous capillary blood and C_{art} represents the arterial glucose concentration.

Equation (6) assumes that the concentration of glucose in abluminal fluid (C_b) is constant along the length of villus capillaries as they descend from the villus tips. Alternatively, it may be supposed that both the blood and abluminal concentrations increase linearly with distance along the capillary length (i.e. constant uptake per unit length). In this case the mean concentration in abluminal fluid (C_{bm}) becomes

$$C_{bm} = \frac{J_S}{\mathrm{PS}} + \frac{(C_V + C_{art})}{2}. \quad (6a)$$

Both eqns (6) and (6*a*) yield the values for C_b within about 10 % of each other over the entire range of glucose loads shown in Table 2.

Equations (3), (4) and (6) contain all the information required to estimate the concentrations of glucose in intercellular channels and the concentration at the abluminal surface of capillaries required to drive any given flux into villus capillary blood. At any given J_S in eqn (3), C_b is determined solely by the properties of the microvascular system (eqn (6)) and the concentrations in intercellular channels produced by the epithelial transport system must equal or exceed its value. Obviously, if the permeability–surface area product (PS) were zero there could be no steady-state absorption: as PS decreases, C_b increases until it exceeds the capacity of the epithelial system to support the condition that $C_a > C_b$. Thus C_b may be regarded as a boundary condition set by the villus microvascular system that may limit the flux attainable by the epithelium (both trans-cellular and paracellular).

When the above equations are entered as formulae in computer spreadsheets (as in Table 2) the effects on predicted concentration gradients of variations in fluxes, villus capillary blood flow and permeability−surface area products can be computed automatically.

Part II: numbers for application to eqns (3), (4) and (6)

Absorption rates from perfused segments of unanaesthetised animals are several times greater than those measured in acute experiments on anaesthetised preparations (Ugolev, 1987). The most extensive measurements in unanaesthetised animals have been made in perfused jejunal segments of rats and normal humans and we have therefore used data from these species for values of glucose flux (J_s) and fluid absorption (J_v). Estimation of the concentration gradients in intercellular channels from eqns (3*b*) and (4) and the concentration in fluid at the abluminal surface of capillaries from eqn (6) requires numerical data for dimensions of channels (r_s, r_b and x_b), P, S (or PS), C_{art} and $\dot{Q}_b$. Complete data for these quantities are not available for any one species; dimensions of intercellular channels between enterocytes during absorption have only been investigated in hamster jejunum (Madara & Pappenheimer, 1987) and villus blood flows ($\dot{Q}_b$) and capillary permeability–surface products (PS) have only been investigated in jejunum of anaesthetised cats (Dresel *et al.* 1966; Svanvik, 1973; Perry & Granger, 1981) or dogs (Bond & Levitt, 1979). The most detailed studies of the surface area, S, of jejunal villus capillaries have been performed in dogs (Mall, 1887), cats (Casley-Smith *et al.* 1975) and rabbits (Vimtrup, 1929). The methods and potential errors involved in transferring data from other species to rats and humans are discussed below in connection with each variable.

Fluxes. The fluxes J_S and J_V, listed in columns A and B of Table 2, are essentially the same as those published previously (Pappenheimer, 2001*a*,*b*). Data from rat jejunum were obtained from perfusion of Thiry-Vella loops in unanaesthetised rats (Gruzdkov, 1993; Gruzdkov & Gromova, 1995; Gromova & Gruzdkov, 1999). Data from humans are average values obtained by several groups of investigators (Holdsworth & Dawson, 1964; Malawer *et al.* 1965; Gray & Inglefinger, 1965, 1966; Fordtran & Saltin, 1967; Sladen & Dawson, 1969; Fordtran, 1975; Gisolfi *et al.* 1992; Fine *et al.* 1993). The fluxes have been normalised to per square centimetre of smooth luminal surface using the conversion factors described by Pappenheimer (1998). Different combinations of J_S and J_V (all within errors of experimental measurement) can be found that result in slightly different values for C_a and C_b but all such combinations have little effect on the calculated concentration gradients in intercellular fluid ($C_a - C_b$).

Surface areas of villi and villus capillaries in jejunum. In rats (Fisher & Parsons, 1950), hamsters (Buschman & Manke, 1981), cats (Casley-Smith *et al.* 1975) and dogs (Mall, 1887) the villus surface is 5–7 cm^2 (cm^2 of smooth luminal surface)$^{-1}$. However, absorption of fluid and solutes takes place principally in the upper third of the villi (Kinter & Wilson, 1965; Lee, 1969; Ugolev, 1989) having a surface of about 2 cm^2 (cm^2 of smooth luminal surface)$^{-1}$. Human jejunal villi are longer and have a larger surface area relative to luminal surface (Madara & Trier, 1994). In the calculations to follow we assume that the absorbing surface of the upper third of human jejunal villi is 3 cm^2 (cm^2 of luminal surface)$^{-1}$. As noted by Krogh (1929) on the basis of histological measurements by Mall in dog jejunum and by Vimtrup in rabbits, the surface area of villus capillaries is 80–90 % of the surface area in the upper third of the villi. These results refer to tissues that had been injected with carbon black and fixed for subsequent examination by light microscopy. It was presumed that the small blood vessels were dilated and that measured surface areas were maximal in the samples examined. Comparable results from villi of cat jejunum were obtained by Casley-Smith *et al.* (1975) using electron microscopy of tissues fixed by glutaraldehyde. Under normal circumstances *in vivo* the functional surface area of the villus capillaries is relatively small in the non-absorbing state and increases in parallel with blood flow during absorption of nutrients as discussed below in the section on permeability–surface area product.

Dimensions of enterocytes and intercellular channels. Sagittal sections from which linear dimensions can be measured are available from non-absorbing enterocytes of hamsters (Buschman & Manke, 1981; Madara & Pappenheimer, 1987), rats (Buschman, 1983) and humans (Madara & Trier, 1994). In sections of non-absorbing jejunum the lateral membranes of enterocytes are so closely apposed that there is little or no measurable

Table 1. Dimensions of jejunal enterocytes of hamster, rat and human used to calculate the cross–sectional area and length of the paracellular pathway

	Non-absorbing				Absorbing			
	r_S	r_b	x_b	V_{cell}	r_S	h	V_{cell}	r_b
Hamster	4.75	4.00	21	1503*	4.75	4	1040*	2.4
Rat	3.65	3.1	28	1181*	3.65	5*	825*	1.9*
Human	5.5	4.80	36	3500*	5.50	6*	2452*	3.0*

Measured values are shown in plain type; * indicates calculated values. All values are given in μm or μm^3, as appropriate. On the basal side of the tight junction, the cells are treated as truncated cones with radii of r_s at the level of the tight junction and r_b at the level of the basement membrane. The height of the cone is x_b and the distance from the brush border to the basal side of the tight junction is h (see Fig. 2*A*). V_{cell}, volume of cell.

intercellular space. During Na^+-coupled absorption of sugars and amino acids the cells shrink and intercellular spaces are easily identified. However, sections from absorbing jejunum are only available from hamsters. Dimensional data from these sections are summarised in the first row of Table 1. Although comparable data from other species are not available, it is nevertheless possible to estimate the dimensions of absorbing cells and channels from measured dimensions of non-absorbing cells on the assumption that the cells lose 30 % of their volume during absorption, as found in hamster jejunum. Following the morphometric studies of rat and hamster enterocytes by Buschman & Manke (1981) we assume that each cell is an inverted truncated cone of height x_b μm having radii of r_s and r_b μm, set on a cylindrical base of height h μm, and radius r_s μm. The volume of each cell is therefore given by:

$$V_{cell} = \pi r_s^2 h + (\pi x_b/3)(r_s^2 + r_s r_b + r_b^2). \quad (7)$$

As shown in the first row of Table 1 the average volume of hamster enterocytes calculated by eqn (7) is 1503 μm^3 in the non-absorbing state and 1040 μm^3 during absorption of glucose. This estimate of volume in the non-absorbing state is not significantly different from that of 1452 ± 103 μm^3 found by Buschman & Manke (1981) who used the more accurate stereological techniques of Weibel & Bolender (1973). Reasons for the loss of about 30 % of cell volume during Na^+-coupled transport have been described previously (Pappenheimer, 2001*b*). Values for r_b during absorption in rats and humans can be estimated from eqn (7) on the assumption that the percentage changes of cell volume are approximately the same as in hamsters. These calculated values are shown in the second and third rows of Table 1, marked with asterisks. Given the dimensions of cells listed in Table 1, the cross-sectional area of the channels (A_x) relative to the cell surface area (A_s) at any distance (x) beneath the tight junction is defined by

$$\frac{A_x}{A_S} = 1 - \left(\frac{(r_S - r_b)(x_b - x)}{r_S x_b} + \frac{r_b}{r_S}\right)^2.$$

As noted above, the cell surfaces facing the lumen are polygonal rather than circular but this geometry has no effect on the estimated values of A_x/A_s of subjunctional intercellular channels.

Weight of villus tissue. Fluxes of solutes and fluid absorption rates for insertion in eqns (1), (3) or (6) are usually expressed per square centimetre of smooth luminal surface whereas available data for intestinal blood flow or permeability–surface area products are expressed per gram tissue. It is therefore necessary to specify the weight of the villi relative to whole jejunum and to utilise the species-specific relations between weight and smooth luminal surface (Table 1 in Pappenheimer, 1998).

The villi account for approximately 15 % of jejunal weight in cats (Svanvik, 1973; Casley-Smith *et al.* 1975) and dogs (Mall, 1887). When expressed per square centimetre of smooth luminal surface the villi weigh approximately 0.03 g in both species. If the same were to be true of rats then each gram of jejunal villus tissue corresponds to about 133 cm^2 of smooth lumenal surface. The relative weight of the villi in human jejunum is greater owing to the numerous villus-covered plicae that extend into the intestinal lumen. Cut-outs from histological sections (Bremer, 1930) indicate that the villus layer accounts for some 30 % of jejunal weight in the adult human. Thus there are 4.8 cm^2 of smooth lumenal surface per gram of human jejunum and 16 cm^2 of smooth luminal surface per gram of villus tissue (Pappenheimer, 1998).

Villus blood flow. Villus blood flow measured with microspheres in anaesthetised dogs increases from 23 ± 10 to 200 ± 30 $cm^3\ min^{-1}$ (100 g villus tissue)$^{-1}$ (means ± S.E.M.) during vasodilatation induced by glucagon (Bond & Levitt, 1979). Values as high as 300 $cm^3\ min^{-1}$ (100 g villus tissue)$^{-1}$ were found in jejunal villi of anaesthetised cats during hyperaemia caused by infusion of isopropylnoradrenaline into the superior mesenteric artery (Biber *et al.* 1973). There are no systematic data relating villus blood flow to rates of glucose absorption but it is known that jejunal blood flow increases during absorption of nutrients. Blood flow measured by Doppler ultrasound in the superior mesenteric artery of human subjects increases from about 250 to 400 $cm^3\ min^{-1}$ after a light meal and to

more than 700 $cm^3\,min^{-1}$ after a large meal (Sidery & MacDonald, 1994). In unanaesthetised dogs Shoemaker *et al.* (1963) found that ingestion of 50 g glucose increased portal blood flow by about 250–350 $cm^3\,min^{-1}$ at a time when the glucose absorption rate was 1.8 mmol min^{-1}. The absorbing regions of the duodenum–jejunum of dogs of 20 kg body weight weigh about 200 g (Pappenheimer, 1998) and according to Svanvik (1973) the villus blood flow per gram of villus tissue is about 1.7 times that of the whole jejunum. Thus, if all the increased portal flow is derived from duodenum–jejunum, the increased blood flow in the experiments of Shoemaker *et al.* was $(300 \times 60)/200 = 90\ cm^3\,h^{-1}$ (g duodenum–jejunum)$^{-1}$ and 152 $cm^3\,h^{-1}$ (g villus tissue)$^{-1}$. A similar post-prandial increase in jejunal blood flow, directed entirely to the absorbing mucosa, was found by Gallavan *et al.* (1980) who used the microsphere technique in conscious dogs to measure regional blood flows before and after feeding. If the same increase in villus blood flow during comparable rates of glucose absorption occurs in the jejunum of rats having a luminal surface area (S_L) of 133 cm^2 (g villi)$^{-1}$ (see Weight of villus tissue, above) then the increased flow may be estimated as $(152/133) = 1.15\ cm^3\,h^{-1}\,(cm^2\ S_L)^{-1}$. In human jejunum having an S_L of 16 cm^2 (g villi)$^{-1}$ the increased flow may be estimated as $(152/16) = 8.7\ cm^3\,h^{-1}\,(cm^2\,S_L)^{-1}$.

Villus blood flow in the non-absorbing ('resting') jejunum has been estimated to be $14 \pm 6\ cm^3\,h^{-1}$ (g villus tissue)$^{-1}$ (mean ± S.E.M.) in anaesthetised dogs (Bond & Levitt, 1979) or anaesthetised cats (Svanvik, 1973). When expressed per square centimetre of S_L this becomes $(14 \pm 6/133) = 0.11 \pm 0.05$ in rat jejunum and $(14 \pm 6/15) = 0.93 \pm 0.4$ in human jejunum. In the absence of further data relating villus blood flow to rates of glucose absorption we assume that the increased flow is proportional to the rate of glucose absorption, $\dot{Q}_b - \dot{Q}_{rest} = kJ_s$, where $\dot{Q}_{rest}$ represents blood flow when J_S is zero and k is the proportionality constant. In rats, $k = (1.15/70) = 0.017$ and in humans $k = (8.7/400) = 0.022$. The standard errors for blood flow were not given in the paper by Shoemaker but the standard errors for portal–arterial blood concentration differences were about ± 20 % of the mean values. For present purposes we assume (within reasonable standard errors) that in rats

$$\dot{Q}_b = 0.11 + 0.018J_S, \qquad (8a)$$

and in humans

$$\dot{Q}_b = 0.9 + 0.02J_S, \qquad (8b)$$

as indicated in column C of Table 2. These indirect estimates of villus blood flow are admittedly based on inadequate experimental evidence; for this reason the principal results are presented in Figs 3, 4, 5 and 6 for a wide range of villus blood flow responses to glucose loading.

Arterial glucose concentration, C_{art}. The concentration of glucose in arterial blood (C_{art}) is normally 5 mM but can rise to 15 mM during absorption of large glucose loads as found in glucose tolerance tests in humans or in dogs loaded with 50 g glucose (Shoemaker *et al.* 1963). For application to eqn (6) we assume that C_{art} increases from 5 to 15 mM in proportion to the glucose load, as shown in column D of Table 2.

The permeability–surface area product, PS. The permeability of capillary beds to test solutes multiplied by the surface area of the capillaries (PS) can be estimated from their arterio–venous extraction ratios (E) at any given blood flow ($\dot{Q}_b$) as described by Renkin (1955) and by Crone (1963). Thus,

$$PS = \dot{Q}_b/\ln(1 - E). \qquad (9)$$

Equation (9) has been applied to jejunal segments in anaesthetised cats by Dresel *et al.* (1966), using ^{86}Rb as test solute and to ileal segments by Perry & Granger (1981) utilising raffinose and inulin. Their results show that PS for lipid-insoluble solutes the size of glucose is about 15 $cm^3\,h^{-1}$ (g intestine)$^{-1}$ at low blood flows, increasing to 36 $cm^3\,hr^{-1}\,g^{-1}$ during maximum vasodilatation induced by infusions of adenosine or isopropylnoradrenaline into the superior mesenteric artery. The relation is given approximately by

$$PS = 0.44\,\dot{Q}_b + 8.6, \qquad (10)$$

where the latter value is expressed as $cm^3\,h^{-1}$ (g intestine)$^{-1}$.

Perry & Granger (1981) point out that because at least 80 % of the resting blood flow of the cat small intestine is directed to the mucosa–submucosa and that this fraction increases with vasodilatation, their estimates of PS reflect the properties of the fenestrated capillaries of the jejunal mucosa. The average smooth luminal surface area (S_L) of the small intestine in cats is 5.0 $cm^2\,g^{-1}$; when $\dot{Q}_b$ and PS are expressed per square centimetre of S_L eqn (9) becomes

$$PS\,(cat) = 0.44\dot{Q}_b + 1.7, \qquad (10a)$$

where the latter value is expressed as $cm^3\,h^{-1}\,(cm^2\,S_L)^{-1}$.

If the same increase of PS with $\dot{Q}_b$ occurs during glucose absorption in rats having a jejunal luminal surface area (S_L) of 20 $cm^2\,g^{-1}$ then

$$PS\,(rat) = 0.44\dot{Q}_b + 0.43, \qquad (10b)$$

where the latter value is expressed as $cm^3\,h^{-1}\,(cm^2\,S_L)^{-1}$.

In human jejunum having an S_L of 4.8 $cm^2\,g^{-1}$

$$PS\,(human) = 0.44\dot{Q}_b + 1.8, \qquad (10c)$$

where the latter value is expressed as $cm^3\,h^{-1}\,(cm^2\,S_L)^{-1}$.

Equations (10*b*) and (10*c*) are employed to estimate the values for PS shown in column F of Table 2.

Table 2. Glucose fluxes and concentrations in the jejunum

A. Rat

A	B	C	D	E	F	G	H	I	J	K
J_S	J_V	$Q_b = 0.11 + 0.018J_S$	$C_{art} = 5.0 + 0.09J_S$	$C_V = C_{art} + J_S/Q_b$	PS = 0.43 + 0.44Q_b	$C_m = C_b - J_S$/PS	C_b	$(1 - e^{-P})$	$C_a - C_b$	C_a
10	0.11	0.29	5.9	40	0.56	28	46	0.012	0.5	47
30	0.21	0.65	7.7	54	0.72	35	77	0.022	1.5	78
40	0.25	0.83	8.6	57	0.80	36	87	0.026	1.9	89
50	0.28	1.01	9.5	59	0.87	38	95	0.029	2.5	97
60	0.30	1.19	10.4	61	0.95	39	102	0.031	3.1	105
70	0.32	1.37	11.3	62	1.03	40	108	0.033	3.7	111

B. Human

A	B	C	D	E	F	G	H	I	J	K
J_S	J_V	$Q_b = 0.9 + 0.002J_S$	$C_{art} = 5.0 + 0.09J_S$	$C_V = C_{art} + J_S/Q_b$	PS = 1.8 + 0.44Q_b	$C_m = C_b - J_S$/PS	C_b	$(1 - e^{-P})$	$C_a - C_b$	C_a
100	0.78	2.9	7.5	42	3.08	28	60	0.079	5.4	66
200	1.15	4.9	10.0	51	3.96	33	84	0.115	10.4	94
250	1.32	5.9	11.3	54	4.40	35	92	0.131	12.7	105
350	1.60	7.9	13.8	58	5.28	38	105	0.156	17.8	122
400	1.72	8.9	15.0	60	5.72	40	110	0.167	20.5	130

J_S, flux of solute; J_V, flow of solvent; Q_b, capillary blood flow; C_{art}, arterial glucose concentration; C_V, glucose concentration in the venous capillary blood; PS, permeability–surface area product; C_m, steady-state mean glucose concentration difference across the villus capillary endothelium; C_b, concentration of glucose at or near the abluminal surface of villus capillaries immediately adjacent to the basement membrane of epithelial cells; C_a, subjunctional glucose concentration in the intercellular channels; p, Péclet number. All values of J_S, J_V, Q_b and PS are (cm^2 smooth luminal surface)$^{-1}$ h^{-1}; concentrations are mM.

An alternative (independent) estimate of PS during absorption of glucose may be made from the relation between coefficients of hydraulic conductivity (L_p) and diffusion permeability to glucose ($P_{d,g}$). It was shown by Michel & Curry (1999) that P_d to lipid-insoluble solutes is directly proportional to L_p in all capillary beds so far investigated. For a solute the size of glucose,

$$P_{d,g} = L_p \times 10^6, \qquad (11)$$

when $P_{d,g}$ is expressed in cm s^{-1} and L_p is in cm^3 s^{-1} dyn^{-1}.

During absorption of glucose the capillary filtration coefficient of the cat jejunum is about 0.26 cm^3 min^{-1} mmHg $^{-1}$ (100 g tissue)$^{-1}$ (Granger *et al.* 1984) and the total surface area of fenestrated capillaries in the tissue is about 7500 cm^2 (Casley-Smith *et al.* 1975). When expressed in cgs units, $L_p = 0.26/(60 \times 1.35 \times 980 \times 7500) = 4.4 \times 10^{-10}$ cm s^{-1} dyn^{-1} and

$$P_{d,g} = 4.4 \times 10^{-4} \text{ cm s}^{-1} = 1.6 \text{ cm h}^{-1}. \qquad (12)$$

This estimate of capillary permeability to glucose is 10–20 times greater than that found in skeletal muscle (Michel & Curry, 1999) and it places intestinal capillaries among the most permeable so far investigated, including fenestrated capillaries of the salivary glands (Mann *et al.* 1979) and of the ascending vasa recta of the renal medulla (Pallone, 1991) where permeability to Na^+ has been reported to be 10^{-3} cm s^{-1}.

The surface area of capillaries in the upper (absorbing) region of villus capillaries is about 29 cm^2 (g jejunum)$^{-1}$ whence PS to glucose estimated from the filtration coefficient (L_p) and morphometric surface area of capillaries in the villus tips is $29 \times 1.6 = 46$ cm^3 h^{-1}. If jejunal blood flow during absorption of glucose is the same in the cat as in the dog (90 ± 15 cm^3 h^{-1} g^{-1}) then the PS estimated from extraction ratios (eqn (9) above) is PS = $0.44 \times (90 \pm 15) + 8.6 = 48 \pm 7$ cm^3 h^{-1}. The close agreement between these two independent methods of estimating PS lends confidence to their application to eqn (6) and to column F of Table 2.

Diffusion coefficient of glucose in intercellular channels. The diffusion coefficients of small hydrophilic solutes through intercellular channels of cultured Madin-Derby canine kidney (MDCK) cells are not significantly different from their free diffusion coefficients (Kovbasnjuk *et al.* 2000). We therefore assume that the same is true of glucose in dilated channels of absorbing jejunal enterocytes.

Part III: results and discussion of results

The principal results are summarised in Table 2A and 2B. The first two columns list the steady-state rates of net glucose absorption, J_S, (μmol h^{-1} cm^{-2}) and net fluid absorption, J_V, (ml h^{-1} cm^{-2}) as measured from segmental perfusions in unanaesthetised rats or humans; these data provide the experimental basis for calculations in the remaining columns. Equations utilised to calculate the

values in each remaining column are entered for insertion in computer spreadsheets, thus enabling readers to examine the effects of altering estimated values of blood flow, permeability–surface area products or other parameters. For example, if the blood flow responses to glucose loading in rats are restricted to 50 % of the values shown, the equation in column C becomes $\dot{Q}_b = 0.11 + 0.009J_S$ and substitution of this equation will automatically re-calculate values for all the remaining dependent variables in Table 2.

The concentration of glucose at abluminal surfaces of villus capillaries. Column H of Table 2 shows the concentrations of glucose at abluminal surfaces of villus capillaries (C_b) as calculated by eqn (6) from values of permeability–surface area product (column F), villus blood flow (column C) and concentrations in villus capillary blood (columns D and E). The abluminal concentrations increase with glucose load to values as high as 108 mM in rat jejunum and 110 mM in human jejunum. These values indicate that high glucose concentrations contribute significantly to the raised tissue osmolality of the villi during glucose absorption (e.g. Hallbäck *et al.* 1991). It is important to note that the high values of interstitial glucose concentration are predicted from measured rates of glucose absorption and the best available estimates of $\dot{Q}_b$ and PS for the villus capillaries. They are independent of the pathways taken by glucose through the epithelium.

As shown in Fig. 3 the rate of increase of C_b diminishes with load owing to the nutrient-induced increase in capillary blood flow and permeability–surface area product. The increased permeability–surface area product (Table 2, column F) has been attributed to opening of new capillaries associated with the hyperaemia (Dresel *et al.* 1966) but flow-induced increased permeability may also be a factor (Montermini *et al.* 2002).

As noted in Villus blood flow, Part II, there are no systematic experimental data relating villus blood flow to glucose flux in unanaesthetised rats or humans and the data shown in Table 2 are necessarily based on data obtained from unanaesthetised dogs and anaesthetised cats. In order to cover a wider range of microvascular responses we have calculated the effects on C_b of a 50 % reduction or a 100 % increase in the responses shown in column C of Table 2 and these are presented in the upper and lower curves of Fig. 3. When blood flow responses are reduced to one half of those shown in Table 2 the abluminal concentration required to maintain the trans-endothelial flux may exceed 150 mM.

The high abluminal concentrations of glucose provide the driving forces required to account for observed trans-endothelial absorption rates but they also may be expected to cause osmotic withdrawal of fluid from blood flowing through the villus tip. Thus the steady-state mean concentration difference across the villus capillary endothelium ($\Delta C_m = J_s/PS$) may be as high as 70 mM in

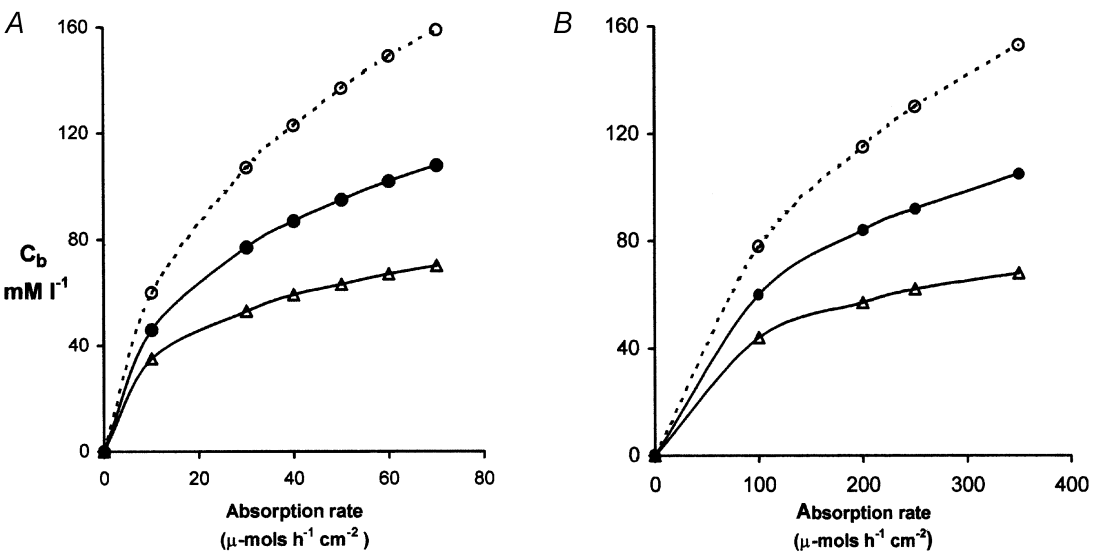

Figure 3. Concentrations of glucose at abluminal surfaces of villus capillaries (C_b): effects of blood flow

A, data from rat showing the relation between C_b and the intestinal absorption rate of glucose (J_S) under three conditions where the increase in villus blood flow (and hence PS) with J_S is either 'normal' (i.e. $\dot{Q}_b = 0.11 + 0.018J_S$ as in Table 2) shown by ● in the middle curve, twice 'normal' (△) or half 'normal' (○). *B*, similar data from human subjects where the 'normal' response is given by $\dot{Q}_b = 0.9 + 0.02J_S$ and the same symbols as in *A* show half 'normal' and twice 'normal' responses.

Table 3. Concentration differences across subjunctional lateral membranes of rat enterocytes

C_L	J_S	J_{SC}	C_a	C_{cell}	$C_{cell} - C_a$
8.5	30	26.5	78	92	14
16	40	33	89	112	23
30	50	38	97	129	32
46	60	42	105	149	44
72	70	44	111	165	54

C_L, mean luminal concentration of glucose; J_S, flux of solvent (from Table 2A); J_{SC}, trans-cellular flux of glucose ($J_{SC} = 48C_L/(C_L + 7)$); C_a, subjunctional glucose concentration in the intercellular channels (from Table 2A); C_{cell}, glucose concentration in the apical cytosol (from eqn (13)).

both rat and human jejunum. Even if the osmotic reflection coefficient to glucose were as low as 0.01 in these highly permeable capillaries, the trans-endothelial osmotic pressures favouring capillary filtration would be about 15 mm Hg, pressures that exceed the Starling forces favouring net absorption of fluid. The central lacteal absorbs some of the fluid reaching the interstitium of the villus lamina propria (Lee, 1969; Granger *et al.* 1984) but the remaining fluid absorption must take place elsewhere, possibly in the extensive capillary bed in the lower two thirds of the villi and surrounding the crypts in the submucosa. This possibility needs to be explored experimentally but wherever the site of fluid absorption may be, the present results show that the large rates of absorption of glucose are made possible by its delivery in high concentration to the abluminal surfaces of the capillaries adjacent to the basement membranes of epithelial cells. During absorption of large glucose loads (e.g. 400 μmol h^{-1} cm^{-2}) the concentration gradient across villus capillary walls is more than 30 times greater than in capillaries of contracting muscle (Vock *et al.* 1996) and the permeability–surface area product is 10–20 times greater than in muscle (Perry & Granger, 1981; Michel & Curry, 1999): these two factors, taken together, can account for the fact that glucose flux across villus capillary walls may be more than 500 times greater than in contracting muscle.

Delivery of glucose from subjunctional fluid to capillaries. The concentrations of glucose (C_b) shown in Fig. 3 and column H of Table 2 provide the boundary conditions for integration of eqns (3*a*) and (3*b*) to evaluate the concentration of glucose in subjunctional fluid (C_a) and the concentration gradient ($C_a - C_b$) in para-cellular channels. Column J of Table 2 and Fig. 4*A* and *B* show solutions for rat and human jejunum. In rat jejunum the concentration of glucose arriving at abluminal surfaces of the villus capillaries (C_b) is never less than 95 % of its concentration at the entrance to intercellular channels (C_a). In human jejunum the corresponding figure is 85 %. These estimates of the differences between C_a and C_b are maximum values based on the assumption that the entire glucose flux through the apical membranes of the enterocytes is discharged into the upper 10 % of the lateral

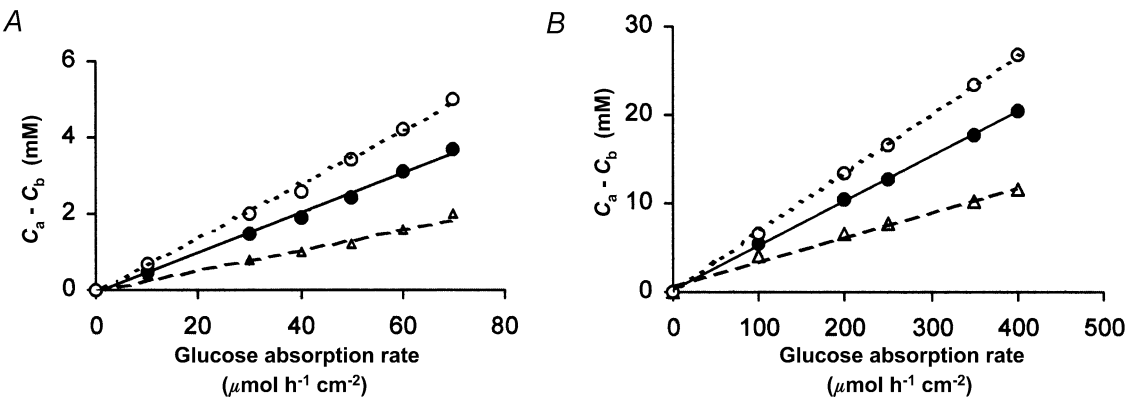

Figure 4. Concentration gradients in the para-cellular channels

Differences in the glucose concentration between the apical and the basal ends of the sub-junctional para-cellular channels in rat (*A*) and human (*B*) are plotted against the rates of glucose absorption. The three lines in each panel show the relations when the vascular response is half normal (○), normal (●), and twice normal (△). If transport of glucose were solely convective, the concentration gradient along the paracellular channel would be zero. Our equations predict small diffusion gradients that are proportional to glucose flux. The concentration of glucose reaching the abluminal surface of the villus capillaries (C_b) is normally within 15 % of its concentration in the subjunctional intercellular fluid (C_a).

intercellular spaces. If the efflux of glucose from the epithelial cells occurs over a larger area of the lateral membranes, $C_a - C_b$ is correspondingly reduced. Thus glucose entering paracellular channels from the epithelial transport system is delivered to capillaries without significant loss of concentration. This conclusion is independent of the details we have assumed for the glucose transport pathway through the epithelial cells.

In two previous analyses of paracellular transport (Pappenheimer & Volpp, 1992; Pappenheimer, 1993) no account was taken of the capillary barrier and a large concentration gradient in paracellular channels leading to capillaries was assumed. These earlier accounts are now superseded by the present analysis.

The concentration gradient across barriers separating the brush border from subjunctional intercellular space; comparison of epithelial with microvascular barriers. Passage of glucose through the cytoplasm of absorptive cells is obstructed by the nucleus, mitochondria and other densely packed membranous structures that occupy most of the cross-sectional area of the cells as described in Part I. Glucose that has been concentrated in the apical cytosol on Na^+-SLGT-1 is therefore discharged to intercellular channels through lateral membranes immediately below the microvilli and cell 'tight' junctions. This is also the site for discharge of Na^+ against its concentration gradient by the Na^+–ATP pump (Ussing & Nedergaard, 1993). The trans-membrane discharge of glucose is generally supposed to occur by facilitated diffusion on Glut-2 that is mobilised to apical membranes during Na^+-coupled glucose transport (Cheeseman, 1992; Kellett, 2001). In the present paper we have shown that at any given flux the concentration of glucose in intercellular fluid bathing lateral membranes is determined primarily by the permeability and blood flow in villus capillaries; it follows that the concentration of glucose in apical cytosol must exceed the intercellular concentration in order to provide the trans-membrane gradient for facilitated diffusion on Glut-2. Although there are no direct measurements of glucose concentration in apical cytosol, an estimate may be deduced from the values of C_a and the properties of the Glut-2 transporter.

Facilitated diffusion on Glut-2 obeys allosteric kinetics with half saturation at about 55 mM and a Hill coefficient of 1.6 (Kellett, 2001). The maximum transport capacity (V_{max}) of Glut-2 in rats fed on a moderate carbohydrate diet is about 15 μmol min^{-1} (mg absorptive cell protein)$^{-1}$ (Cheeseman & Harley, 1991). Since absorptive cell proteins comprise about 10 % of cell weight (Kimmich, 1975) or about 1 % of jejunal weight and 1 g of rat jejunum has a smooth luminal surface area of 20 cm^2 (Pappenheimer, 1998), the V_{max} may be estimated as about 450 μmol h^{-1} (cm^2 smooth luminal surface)$^{-1}$. Given these properties of Glut-2 and the trans-cellular flux (J_{SC}) as a function of mean luminal concentration C_L, it is then possible to estimate the concentrations in apical cytosol (C_{cell}) from the relation:

$$J_{SC} = 450\left(\frac{C_{cell}^{1.6}}{C_{cell}^{1.6} + 55^{1.6}} - \frac{C_a^{1.6}}{C_a^{1.6} + 55^{1.6}}\right). \qquad (13)$$

In the steady state the lateral membrane flux equals the apical membrane flux that has been determined experimentally as $48C_L/(C_L + 7)$ by Gromova & Gruzdkov (1999) and C_a is taken from the results listed in Table 2 (column K) of the present paper. Table 3 shows C_{cell} and the concentration differences across subjunctional lateral membranes ($C_{cell} - C_a$) calculated as above from the properties of Glut-2 and our estimates of C_a in subjunctional intercellular fluid when capillary blood flow and permeability–surface area product are in the normal range shown in Table 2. Since our estimates of V_{max} are based on limited experimental data, the absolute values of C_{cell} in Table 3 are uncertain. C_{cell}, however, must always be greater than C_a and as a consequence of the non-linear

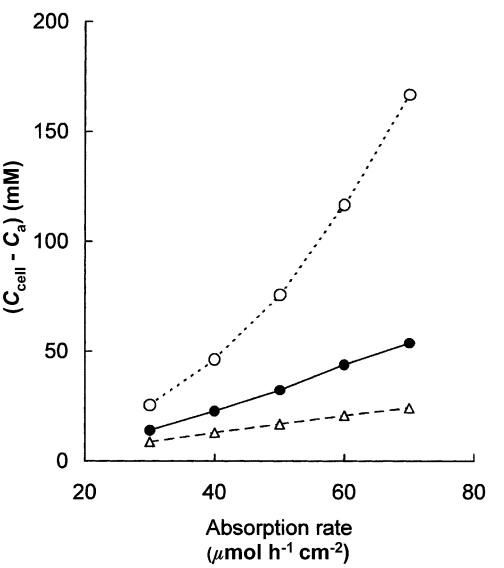

Figure 5. Concentration differences across subjunctional lateral membranes of rat enterocytes during absorption of glucose

At glucose absorption rates greater than 30 μmol h^{-1} cm^{-2}, the predicted concentration differences across subjunctional lateral membranes of rat jejunal enterocytes increase with absorption rate. The three curves show the relations when the vascular response to glucose loading is half normal (○), normal (●) and twice normal (△). When the normal increase in $\dot{Q}_b$ and PS is halved, the concentration in the subjunctional intercellular fluid exceeds 160 mM when the glucose flux is 70 μmol h^{-1} cm^{-2} so that to maintain the flux, the apical cytosolic concentration exceeds 300 mM (see Figs 3 and 4). Such high intracellular concentrations may be expected to diminish the apical influx on SGLT-1 and under these conditions of low blood flow the villus microvascular system limits the rate at which epithelial transport can be sustained.

kinetics of transporters, $(C_{cell} - C_a)$ is likely to increase with J_S in a similar way to that shown in Table 3. Thus a negligible difference in concentration across the lateral membranes at low glucose fluxes becomes a substantial difference if high fluxes are achieved in absence of increases in $\dot{Q}_b$ and PS.

The effects of variations in the microvascular response to glucose loading upon the relations between $(C_{cell} - C_a)$ and J_S are shown in Fig. 5. When the increase in $\dot{Q}_b$ with J_S is normal or doubled, $(C_{cell} - C_a)$ is seen to increase approximately linearly with J_S and the slope of this relation is inversely proportional to the increase in villus blood flow. When the increase in blood flow with absorption rate is halved, however, the increase in $(C_{cell} - C_a)$ with J_S is not only greater than at normal $\dot{Q}_b$, but rises exponentially with J_S. While the trans-cellular flux J_{SC} becomes nearly constant as SGLT-1 approaches saturation (Table 3), larger and larger values of $(C_{cell} - C_a)$ are required to maintain J_{SC} in the face of a rising C_a.

We have shown that, at any level of J_S, the glucose concentration in the lateral intercellular spaces is largely determined by the blood flow through the villus capillaries and the product of their permeability and surface area. From Fig. 5 we now see that the microcirculation may profoundly influence the glucose concentration in the epithelial cells. With the increases in $\dot{Q}_b$ (and hence PS) that were used in Table 2A, C_{cell} must rise to 180 mM when glucose absorption rate is 70 μmol h^{-1} cm^{-2}. If glucose absorption could be sustained at this rate when the microvascular response was halved, C_{cell} would exceed 300 mM. From this calculation it is not difficult to see how easily failure of the microcirculation would compromise the efficiency of SGLT-1 upon which all glucose absorption depends. Our analysis predicts that if the increase in villus blood flow accompanying absorption were inhibited, the absorption rate of glucose would be greatly impaired.

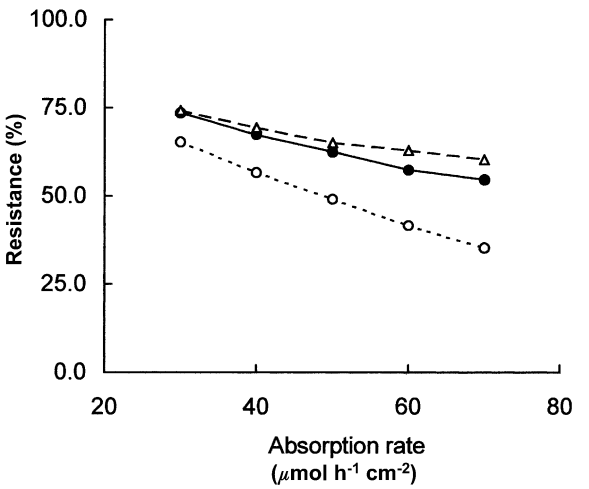

Figure 6. The capillary barrier to absorption of glucose in the rat jejunum

Resistance of the capillary barrier as a fraction of total resistance to glucose transport between apical cytosol and villus capillary blood estimated as the ratio of the mean concentration difference across capillary walls to the mean concentration difference between the apical cytosol and the capillary blood, $(C_b - C_m)/(C_{cell} - C_m)$, has been expressed as a percentage and plotted against the glucose absorption rate under conditions when the microvascular response was normal (●), 50 % of normal (○) and twice normal (△). It is seen that the capillaries account for between 50 and 75 % of the resistance to absorption of glucose at normal physiological blood flows and glucose loads.

Figures 3, 4 and 5, the data in columns G, H and K of Table 2A and the values of C_{cell} in Table 3 provide the information needed to estimate the relative resistances of the epithelial and capillary barriers to absorption of glucose in unanaesthetised rats. Thus at any given flux J_S the resistance of the capillary barrier relative to the overall resistance is given by

$$R_{cap} = (C_b - C_m)/(C_{cell} - C_m). \quad (14)$$

Figure 6 shows that the resistance of capillary barriers calculated from eqn (14) is normally between 50 % and 75 % of the total resistance at all physiological blood flows and glucose loads. We therefore conclude that responses of the villus microvascular system, including increases in blood flow and permeability–surface area product with increasing nutrient load, play a major (and previously unrecognised) role in the absorption of nutrients. That the capillaries in each gram of villus tissue have the capacity to absorb extraordinarily large loads of nutrients is beyond dispute. In the present paper we have described mechanisms that can account quantitatively for this capacity in terms of known permeability properties of capillary endothelium and the microvascular responses to glucose loading. Potential chemical or neurohumoral signals from the epithelial transport system that trigger the necessary microvascular responses include hypertonic NaCl (Bohlen, 1982) and adenosine (Sawmiller & Chou, 1992).

APPENDIX

Derivation of eqn (4); integration of the variable Péclet number

With reference to Fig. 2*A*, at any level, x, beneath the tight junction, the radius of the cell, r_x, is:

$$r_x = ((r_s - r_b)(x_b - x)/x_b) + r_b. \quad (A1)$$

The cross-sectional area of the channels (A_x) at any distance (x) is defined by the cross-sectional area of the cell surface $(\pi r_s)^2$ less the cross-sectional area of the cells at distance x.

$$A_x = \pi r_s^2 - \pi[(r_s - r_b)(x_b - x)/x_b + r_b]^2$$

or

$$A_x/A_s = 1 - [(r_s - r_b)(x_b - x)/r_s x_b + r_b/r_s]^2. \quad (A2)$$

Let

$$z = (r_s - r_b)(x_b - x)/r_s x_b + r_b/r_s,$$

whence,

$$dz = -[(r_s - r_b)/r_s x_b]dx \text{ and } A_x/A_s = 1 - z^2.$$

The integral of the variable Péclet number (eqn (3) of text) can then be expressed by:

$$p = \frac{J_V}{D}\frac{r_S x_b \times 10^{-4}}{2(r_S - r_b)}\ln\left(\frac{(1 - z_b)(1 + z_a)}{(1 + z_b)(1 - z_a)}\right), \qquad (A3)$$

when $x = x_b$, $z_b = r_b/r_s$ and

$$(1 - z_b)(1 + z_b) = (r_s - r_b)/(r_s + r_b),$$

when $x = x_a$, $z_a = 1 - (r_s - r_b)x_a/r_s x_b$ and

$$(1 + z_a)(1 - z_a) = [2r_s x_b - (r_s - r_b)x_a]/(r_S + r_b)x_b,$$

whence substitution in eqn (A3) yields eqn (4) of the text:

$$p = \frac{J_V r_S x_b \times 10^{-4}}{2D(r_S - r_b)}\ln\left(\frac{(2r_S x_b - (r_S - r_b)x_a)}{(r_S + r_b)x_a}\right). \qquad (4)$$

Numerical example for human jejunum

$D_{glucose} = 0.032$ cm^2 h^{-1}, $r_S = 5.5$, $r_b = 3.0$, $x_b = 36$ μm and $x_a = 0.1x_b = 3.6$ μm,

$$p = [(5.5)(36)(10^{-4})J_v/(0.032)(2)(5.5 - 3.0)]\ln \{[(2)(5.5)(36) - (2.5)(3.6)]/(5.5 - 3.0)(3.6)\} = 0.314\,J_v.$$

J_v refers to 1 cm^2 of absorptive cell surface. In human jejunum the cell surface is about 3 times that of the smooth luminal surface of the intestine (see text) so if J_V and J_S refer to luminal surface as in columns A and B of Table 2 then $p = 0.314\,J_V/3 = 0.105 J_V$.

REFERENCES

Amerongen HM, Mack JA, Wilson JM & Neutra MR (1989). Membrane domains of intestinal epithelial cells: distribution of Na^+, K^+-ATPase and the membrane skeleton in adult rat intestine during fetal development and after epithelial isolation. *J Cell Biol* **109**, 2129–2138.

Biber B, Lundgren O & Svanvik J (1973). Intramural blood flow and blood volume in the small intestine of the cat as analyzed by an indicator dilution technique. *Acta Physiol Scand* **87**, 391–403.

Bohlen HG (1982). Na^+-induced intestinal interstitial hyperosmolality and vascular responses during absorptive hyperemia. *Am J Physiol* **242**, H785–789.

Bond JH & Levitt MD (1979). Use of microspheres to measure small intestinal villus blood flow in the dog. *Am J Physiol* **236**, E577–583.

Bremer JL (1930). *A Textbook Of Histology*, Fig 236, P274 P. Blakiston Son & Co., Inc., Philadelphia.

Buschman RJ (1983). Morphometry of the small intestinal enterocytes of the fasted rat and the effects of colchicines. *J Cell Tissue Res* **231**, 289–299.

Buschman RJ & Manke DJ (1981). Morphometric analysis of the membranes and organelles of the small intestinal enterocytes I. Fasted hamster. *J Ultrastruct Res* **76**, 1–14.

Casley-Smith JR, O'Donoghue PJ & Crocker KWJ (1975). The quantitative relationship between fenestrae in jejunal capillaries and connective tissue channels: proof of 'tunnel capillaries'. *Microvasc Res* **9**, 7–100 .

Chang MH (2002). The magnitude and significance of passive absorption in intact house sparrows, *Passer domesticus*. PhD Dissertation, University of Wisconsin-Madison.

Cheeseman CI (1992). Role of intestinal basolateral membrane in absorption of nutrients. *Am J Physiol* **263**, R482–488.

Cheeseman CI & Harley B (1991). Adaptation of glucose transport across rat enterocyte basolateral membranes in response to altered dietary carbohydrate intake. *J Physiol* **437**, 563–575.

Crone C (1963). The permeability of capillaries in various organs as determined by the indicator dilution method. *Acta Physiol Scand* **58**, 292–305.

Dainty J & House CR (1966). 'Unstirred' layers in frog skin. *J Physiol* **182**, 66–78.

Denbigh KG (1965). *Chemical reactor theory*, p. 54. Cambridge University Press, Cambridge, UK.

Dill DB, Edwards HT & Talbott JH (1932). Studies in muscular activity. *J Physiol* **77**, 49–62.

Dresel P, Folkow B & Wallentin I (1966). Rubidium clearance during neurogenic redistribution of intestinal blood flow. *Acta Physiol Scand* **67**, 173–184.

Fine KD, Santa Ana CA, Porter JL & Fordtran JS (1993). Effect of D-glucose on intestinal permeability and its passive absorption in human small intestine *in vivo*. *Gastroenterol* **105**, 1117–1125.

Fisher RB & Parsons DS (1950). The gradient of mucosal surface area in the small intestine of the rat. *J Anat* **84**, 272–282.

Fordtran JS (1975). Stimulation of active and passive sodium absorption by sugars in the human jejunum. *J Clin Invest* **55**, 728–737.

Fordtran JS & Saltin B (1967). Gastric emptying and intestinal absorption during prolonged severe exercise. *J Appl Physiol* **23**, 331–335.

Gallavan RH, Chou CC, Kvietys PR & Sit SP (1980). Regional blood flow during digestion in the conscious dog. *Am J Physiol* **238**, H220–225.

Gisolfi CV, Summers RW, Schedl HP & Bleiler Tl (1992). Intestinal water absorption from select carbohydrate solutions in humans. *J Appl Physiol* **73**, 2142–2150.

Granger DN, Perry MA, Kvietys PR & Taylor AE (1984). Capillary and interstitial forces during fluid absorption in the cat small intestine. *Gastroenterol* **86**, 267–273.

Gray GM & Inglefinger FJ (1965). Intestinal absorption of sucrose in man: the site of hydrolysis and absorption. *J Clin Invest* **44**, 390–397.

Gray GM & Inglefinger FJ (1966). Intestinal absorption of sucrose in man: interrelation of hydrolysis and monosaccharide product absorption. *J Clin Invest* **45**, 388–397.

Gromova LV & Gruzdkov AA (1999). Hydrolysis-dependent absorption of disaccharides in the rat small intestine (chronic experiments and mathematical modeling). *Gen Physiol Biophys* **18**, 209–224.

Gruzdkov AA (1993). Modern concepts of substance transfer across the pre-epithelial layer of the small intestine. *Sech J Physiol* **79**, 19–32 (in Russian).

Gruzdkov AA & Gromova LV (1995). The coupling of disaccharide hydrolysis with absorption of released glucose in the small intestine *in vivo*. *Dokl Akad Nauk* **342**, 830–832 (in Russian).

Gruzdkov AA, Gusev V & Ugolev AM (1989). Mathematical modeling. In *Membrane digestion: new facts and concepts*, ed. Ugolev AM, pp. 228–234. Mir Publishers, Moscow (English edition).

Hallbäck DA, Jodal M, Mannischeff M & Lundgren O (1991). Tissue osmolality in intestinal villi of four mammals *in vivo* and *in vitro*. *Acta Physiol Scand* **143**, 271–277.

Holdsworth CD & Dawson AM (1964). The absorption of monosaccharides in man. *Clin Sci* **27**, 371–379.

Karasov WH & Cork SJ (1994). Glucose absorption by a nectiverous bird: the passive pathway is paramount. *Am J Physiol* **267**, G18–26.

Kellett JL (2001). The facilitated component of intestinal glucose absorption. *J Physiol* **531**, 585–595.

Kety SS & Schmidt CF (1948). The nitrous oxide method for the quantitative determination of cerebral blood flow in man: theory, procedure and normal values. *J Clin Invest* **27**, 476–483.

Kimmich GA (1975). Preparation and characterization of isolated intestinal epithelial cells and their use in studies of intestinal transport. *Methods Membr Biol* **5**, 51–115. Plenum Press, New York.

Kinter WB & Wilson TH (1965). Autoradiographic study of sugar and amino acid absorption by everted sacs of hamster intestine. *Cell Biol* **25**, 19–39.

Koefoed-Johnsen V & Ussing HH (1953). The contributions of diffusion and flow to the passage of D_2O through living membranes. *Acta Physiol Scand* **28**, 60–76.

Kovbasnjuk ON, Bungay PM & Spring KR (2000). Diffusion of small solutes in the lateral intercellular spaces of MDCK cell epithelium grown on permeable supports. *J Memb Biol* **175**, 9–16.

Krogh A (1929). *The Anatomy and Physiology of Capillaries,* 2nd edn, pp. 341–345. Yale University Press, New Haven, USA.

Lee JS (1969). A micropuncture study of water transport by dog jejunal villi *in vitro*. *Am J Physiol* **217**, 1528–1533.

Madara JL & Pappenheimer JR (1987). The structural basis for physiological regulation of paracellular pathways in intestinal epithelium. *J Memb Biol* **100**, 149–164.

Madara JL & Trier JG (1994). The functional morphology of the mucosa of the small intestine. In *Physiology of the Gastrointrestinal Tract*, ed. Johnson LR, chap. **45**. Raven Press, New York.

Malawer SJ, Ewton M, Fordtran JS & Ingelfinger FJ (1965). Interrelationships between jejunal absorption of sodium, glucose and water in man. *Am Soc Clin Invest* **44**, 1072 –1073.

Mall JP (1887). Die Blut und Lymphwege im Dünndarm des Hundes. *Abhandlung der Mathematische-Physischen Classe der Königl Sächsischen Gesellschaft der Wissenschaften* XIV pp. 153–189.

Mann GE, Smaje LH & Yudilevich DL (1979). Permeability of the fenestrated capillaries in the cat submandibular gland to lipid-insoluble molecules *J Physiol* **297**, 335 – 354.

Michel CC & Curry FE (1999). Microvascular permeability. *Physiol Rev* **79**, 703–761.

Montermini D, Winlove CP & Michel CC (2002). Effects of perfusion rate on permeability of frog and rat mesenteric microvessels to sodium fluorescein. *J Physiol* **543**, 959–975.

Nadel ER & Bussolari SE (1988). The Daedalus Project: physiological problems and solutions. *Am Scient* **76**, 351–360.

Nusrat A, Turner JR & Madara JL (2000). Molecular physiology and pathophysiology of tight junctions IV. Regulation of tight junctions by extracellular stimuli: nutrients, cytokines and immune cells. *Am J Physiol* **279**, G851–857.

Pallone TL (1991). Transport of sodium chloride and water in rat ascending vasa recta. *Am J Physiol* **261**, F519 – 525.

Pappenheimer JR (1993). On the coupling of membrane digestion with intestinal absorption of sugars and amino acids. *Am J Physiol* **265**, G409–417.

Pappenheimer JR (1998). Scaling of dimensions of small intestines in non-ruminant eutherian mammals and its significance for absorptive mechanisms. *Comp Biochem Physiol A* **121**, 45–58.

Pappenheimer JR (2001*a*). Role of pre-epithelial 'unstirred' layers in absorption of nutrients from the human jejunum. *J Memb Biol* **179**, 185–204.

Pappenheimer JR (2001*b*). Intestinal absorption of hexoses and amino acids: from apical cytosol to villus capillaries. *J Memb Biol* **184**, 233–239.

Pappenheimer JR & Reiss KZ (1987). Contribution of solvent drag through intercellular junctions to absorption of nutrients by the small intestine of the rat. *J Memb Biol* **100**, 123–136.

Pappenheimer JR & Volpp K (1992). Transmucosal impedance of small intestine: correlation with transport of sugars and amino acids. *Am J Physiol* **263**, C480–493.

Perry MA & Granger DN (1981). Permeability of intestinal capillaries to small molecules. *Am J Physiol* **241**, G24–30.

Renkin EM (1955). Effects of blood flow on diffusion kinetics in isolated perfused hindlegs of cats. A double circulation hypothesis. *Am J Physiol* **183**, 125–136.

Sadowski DC & Meddings JB (1993). Luminal nutrients alter tight-junction permeability in the rat jejunum: an *in vivo* perfusion model. *Can J Physiol Pharmacol* **71**, 835–839.

Sawmiller DR & Chou CC (1992). Role of adenosine in postprandial and reactive hyperemia in canine jejunum. *Am J Physiol* **263**, G487–493.

Shoemaker WC, Yanof HM, Turk IM III & Wilson TH (1963). Glucose and fructose absorption in the unanesthetized dog. *Gastroenterology* **44**, 654–663.

Sidery MB & MacDonald IA (1994). The effect of meal size on the cardiovascular responses to food ingestion. *Br J Nutr* **71**, 835–848.

Sladen GE & Dawson AM (1969). Interrelationships between the absorption of glucose, sodium and water by the normal human jejunum. *Clin Sci* **36**, 119 – 132.

Svanvik J (1973). Mucosal blood circulation and its influence on passive absorption in the small intestine. An experimental study in the cat. *Acta Physiol Scand Suppl* **385**, 1–44.

Ugolev AM (1987). Membrane transport and hydrolytic enzymes under physiological *vs.*acute experimental conditions. *News Physiol Sci* **2**, 186–190.

Ugolev AM (1989). *Membrane digestion: new facts and concepts.* (English translation). Mir Press, Moscow.

Ussing HH & Nedergaard S (1993). Recycling of electrolytes in small intestine of toad. In *Isotonic Transport in Leaky Epithelia*. Alfred Benzon Symposium, ed. Ussing HH, Fischbarg J, Sten-Knudsen O, Larsen EH & Willumsen NJ, pp. 25–34. Munksgaard Press, Copenhagen.

Vimtrup BJ (1929). Cited In Krogh A. *The anatomy and physiology of capillaries*, 2nd edn, pp. 38–40. Yale University Press, New Haven.

Vock R, Weibel ER, Hoppeler H, Weber JM & Taylor CR (1996). Structural basis of vascular substrate supply to muscle cells. *J Exp Biol* **199**, 1675–1688.

Weibel ER & Bolender EP (1973). Stereological techniques for electron microscopic morphometry. In *Principles and Techniques of Electron Microscopy*, ed. Hayat MA, pp. 237–296. Van Nostrand Reinhold Co., New York.

Acknowledgements

We thank Professors F. E. Curry and E. M. Renkin for helpful suggestions and Drs A. Gruzdkov and L. Gromova for English translations of their 1995 and 1999 papers.

Author's present address

J. R. Pappenheimer: Apartment 113, 66 Sherman Street, Cambridge, MA 02140, USA.